STRUCTURAL AND SPECTRAL STUDIES OF SUNSPOTS

Grant NGR 39-005-066
Supplement No. 5

NATIONAL AERONAUTICS AND SPACE ADMINISTRATION

Annual Report

Period: September 1, 1972 - September 1, 1973

Principal Investigator: Arne A. Wyller

Bartol Research Foundation
of
The Franklin Institute
Swarthmore, Pennsylvania 19081

Submitted: October 3, 1973

TABLE OF CONTENTS

I. Summarizing Introduction

During the first year of operation a number of solar observing programs have been initiated at the Bartol Coudé Observatory. Special attention has been paid to multicolor photometry of umbral cores and the residual intensity midway between the Na D_1 and D_2 lines. Both these observational programs aim at the improvement of present umbral atmospheric models and also test the relation between models and umbral area.

The first photoelectric scan ever performed across the Na D_2 line has been carried out with our newly completed magnetometer. The expected sign reversal between left-hand and right-hand circularly polarized light across the line profile has been demonstrated. The signal difference was smaller by an order of magnitude than the values predicted by Yun (4-6%) but we hypothesize that this may have been due to the large entrance aperture (6") used for the scan on the smallish spot (A_u = 60). This hypothesis has been confirmed by observations of a second spot (A_u = 30) using smaller pinholes. In the latter case, the difference between right and left polarization rose to +6.6% at $\Delta\lambda$ =+0.17Å, and fell to -6.4% at $\Delta\lambda$ = -0.17Å.

Extensive theoretical work has also been carried out during the past year. Among the most notable achievements has been the work of Mullan and Yun on the generation of umbral flashes and penumbral running waves, and the work by Mullan on sunspot

interior models with Alfvén wave emission.

In the subsequent sections the various programs outlined above will be discussed in detail.

II. Observational Work with the Bartol Coudé Telescope

a. Seven Color Photometry of Umbral Cores

The first scientifically significant observations with our new telescope installation at Bartol were carried out during three observing runs on October 20, 26 and 31, 1972. On the first of these runs a smallish spot was observed ($A_u = 60 \cdot 10^{-6}$ S.H.) and the two other runs pertained to a more complex umbra with total umbral area of $80 \cdot 10^{-6}$ S.H. In the latter umbra, - shaped like a 3-foil leaf, - a distinct intensity minimum was found in one leaf near the umbral wall and observed on October 26. Four days later weather again permitted observations but this time the previously observed foil had disappeared and our observations centered on a new minimum in continuum intensity and this time found in the second remaining foil.

We tentatively identify these minima in continuum - intensities with umbral cores described by Bray and Loughhead (1965) in their monograph on sunspots (see p. 132). From their iso-densitometry of short exposure photographs of sunspot umbrae they conclude that these cores are only a few seconds of arc in diameter and their temperature may be as much as 500°K less than

that of the rest of the umbra.

With our larger solar image, 5 inches in diameter, the entrance pinhole aperture of 50 microns corresponds to 0.''8 in diameter, which then would take in a pure sampling of the umbral core intensity. Pulse counting photometry was carried out in the continuum monitor channel of URSIES with various filters centered at respectively λλ3942, 4205, 4538, 4949, 5745, 6529 and 6594 in the echelle mode of the instrument (no interferometer in).

Aureole observations were carried out on the days of observation and scattered light corrections were applied in the traditional manner (see section Id). Because of the extended band passes of the filters carefully worked out corrections had to be applied to the measurements for differential line absorption in the umbral spectrum and the solar disk spectrum. Data were kindly made available by Dr. Wöhl of the Göttingen Observatory for wavelengths longward of λ4500. For the shorter wavelengths recourse was had to line absorption factors from Arcturus (K2III) (Milford, 1950) and unpublished observations by Dr. J. Hershey of the Sproul Observatory on the MOV star BD + 50°1725 and KOV star 70 Ophiuchi.

The resulting umbral to disk center continuum intensities are displayed in Figure 1. Only the results for the two distinct umbral cores observed in the larger spot October 26 and 30 have been plotted. The observations on October 20, while exhibiting a similar run in the curve, in particular the intensity dip at

4949, shows lower values in general, which may in part be due to uncertainities in the scattered light corrections.

It is gratifying to see the close agreement between the intensity curves for the two different umbral cores in the same spot but observed on two different days. The pronounced dip in the curves is difficult to explain. Stumpff (1961) had noticed a similar dip but the Göttingen observers (Wöhl, private communication) did not observe such an effect. Since the observations have been carried out with relatively broad band filters they should be repeated with the narrow band channel. Upon learning of these results Dr. Mattig at the Fraunhofer Institute in Freiburg is planning to undertake such observations this summer.

The excellent agreement between our results and those of Mattig (1971) we take as an indication that our telescope equipment at our new observatory is operating satisfactorily. We are greatly aided by the jog mode of one second of arc steps in the siderostat drives, which enable us to search out the umbral core location in the sunspot umbrae.

While the narrow band continuum observations of February 28 fits comfortably to those of October 26 and 30, the discordant broad and narrow band observations of July 6 and 7 point to problems in aureole corrections which merit further discussion.

In Figure 1 we see the July 6 and 7 observations plotted for various assumptions on the magnitude of the Zwaan factor

(= ratio of scattered light at the location of the spot to scattered light one arc minute from the limb). The value 5.7 was chosen on the basis of the narrow band photometry at the sodium D lines on February 28, 1973 (see section Ib). A complete aureole was obtained at 4920 A (see below) but for the moment we will discuss the results obtained by assuming that Z = 5.7 is appropriate at all wavelengths.

The July spot is significantly brighter than the spots observed last October. However, there is a large difference between the broad-band intensity at 5900Å (observed July 6) and the narrow-band intensity at the D lines (observed July 7). It is not clear why this is so. Perhaps the Zwaan factor for the narrow band observations must be reduced below 5.7. In order to agree with the broad observations, Z (narrow) should be reduced to 2.9, in which case the maximum intensity between the sodium D lines would increase to 0.69. In that case, none of the models in Figure 1 would fit both line and continuum observations at the D lines. It seems better to assume that the narrow band data are correct, with Z = 5.7, for this leads to agreement with one of the models (Kneer's) in <u>both</u> line and continuum. The question then arises as to why the broad-band data are so much brighter. Part of the answer may be that seeing conditions were sufficiently different between July 6 (when the broad-band data were obtained) and July 7 (when the narrow-band data were obtained).

The Zwaan factor for the broad-band data might exceed 5.7. In order to bring the broad-band observations made with the 5900Å filter into equality with the narrow-band observations at 5893Å (and we assume that Z = 5.7 is correct for the latter), it is necessary to take Z = 6.9. (This value will be further justified below.) If Z = 6.9, the umbral intensity relative to the disk becomes:

λ(Å)	4200	4500	4920	5900	6750
I_u/I_d	5.44% 9.17%	2.58% 3.06%	4.42%	9.48%	16.69%

The two values in the short-wavelength bands refer to line corrections taken from the M0 V star (top line) and Arcturus (bottom line).

Returning now to the derivation of the Zwaan factor from the aureole observed at 4920 Å, Figure 2 shows the observations with a theoretical curve fitted to the observations. (Vertical error bars on the observations are small, less than 1%). The theoretical curve suggests that the Zwaan factor has the enormous value of 8.7. This value is however extremely sensitive to the observed point in the aureole closest to the limb of the sun and it violates the upper limit of 7.75 obtained from both our earlier observations at Bartol and Mattig's (1971) aureole (see section Id). Our method of measurement is such that Δ = 1 mm is the closest distance beyond the limb at which we can make aureole observations

with reliability. At distances less than Δ = 1 mm ($\equiv$ 15.8 arc sec at the focal plane of the Bartol instrument) it would be difficult to guarantee accuracy in the distance Δ between the entrance pinhole and the limb. As an indication of how sensitive the Zwaan factor is to the point at Δ = 1 mm, suppose this distance were in error by $\delta\Delta$ = 0.5 mm, so that the largest intensity plotted in Figure 13 actually applies to R/R_o = 1.0087 rather than to 1.0175, as plotted. Then the steeply rising part of the aureole near the limb would become less steep, and the Zwaan factor would fall to 4.3. A value of Z = 6.9, as used above, would be appropriate if the largest intensity plotted in Figure 13 actually applies to R/R_o = 1.014 instead of 1.0175. This corresponds to an error in placing the pinhole relative to the limb of only $\delta\Delta$ = 0.2 mm. Since we use a pinhole with radius 0.2 mm when measuring aureole intensities, it is indeed possible that an error of just this amount could have entered into the measurements. An error in Δ of as much as 0.5 mm is not as probable, and so Z = 4.3 is to be considered a firm <u>lower</u> limit on the true Z factor. We conclude that Z = 6.9, as used above in order to achieve agreement between broad-band and narrow-band intensities near the D lines, is consistent with the aureole observations.

b. Photoelectric Determinations of the Sodium D Wing Intensities in Sunspots

On February 28, 1973 a sunspot of umbral area A_u = 30 was observed with the Bartol spectrometer. The umbral core was observed in three wavelengths using the narrow-band channel, with an exit pinhole of 0.16Å. The wavelengths were 5874.10, 5893.4, and 5931.75. The first and third of these are listed by Wöhl (1970) as locations of clear continuum in spots. The wavelength 5893.4Å lies between the sodium D lines, as close to the mid-point between the lines as is permitted by other lines. The wavelength chosen appears to lie in a range of wavelengths where no faint spectral lines are visible in the Göttingen umbral atlas, so all of the absorption there can be considered to be due to the overlapping wings of the sodium D lines.

Scattered light was determined by measuring the aureole intensity off the north limb at 5931Å, out to a radial distance of 1.77 solar radii. Theoretical aureoles were fitted to the observations and these were very similar to the aureoles fitted to the aureoles observed in October, 1972. The Zwaan factor Z(= ratio of scattered light at location of spot to scattered light one arc minute from the limb) was found to be 5.7 in the best fit. The error bars on the aureole allow Z to be as small as 4.3. The upper limit on Z is 7.75. This is the upper limit set by Mattig's (1971) observation of Mercury's transit (cf. discussion

of scattered light corrections in Section Id).

Using Z = 5.7, the ratio of sunspot intensity to solar disk center intensity was found to be

λ	5874Å	5893.4Å	5931Å
I_*/I_o	8.04%	4.78%	8.78%

The interpolated continuum intensity at 5893.4 is 8.29%. This is to be compared with the broad-band continuum intensity of 7.22% and 7.37% observed in the core of a spot with A_u = 80 on October 26 and 30, 1972. These broad-band measurements were obtained with a filter having peak transmission at 5745Å and effective wavelength (assuming a flat spectrum) of 5826Å. In Figure 1, these observations are plotted at the peak wavelength 5745Å. The dot at 5893Å represents the narrow band continuum intensity observed in the spot with A_u = 30 on February 28, 1973. It appears that this observation lies close to the lines drawn through the observations of October 1972. From this it appears that our procedure for correcting broad-band observations of sunspots for line blanketing is essentially correct, at least in the neighborhood of 5500-6000Å.

Returning now to the table above, and to the intensity between the sodium D lines, the intensity in terms of the local continuum is r = 4.78/8.29 = 0.577. The error bars on this extend to 0.628 (with Z = 4.3, the minimum value) and 0.471

(with Z = 7.75). Figure 3 shows these error bars on the best estimate.

On July 7, 1973, a spot with A_u = 60 was observed at cosθ=0.89. Assuming that the Zwaan correction factors again span the range from Z = 4.3 to 7.75 (the scattered light is largely instrumental, and should remain unchanged in shape at different times), we find that the continuum intensity interpolated at 5893.4Å is 9.53% of the continuum of the sun (assuming Z = 5.7). This is 15% greater than the value observed in the spot on Feb. 28, 1973. The continuum on July 7, 1973 could be reduced to the value observed on Feb. 28, 1973, if Z were as large as 6.8 on July 7, and equal to 5.7 on Feb. 28. It is not clear why Z should vary in this way, and the safest assumption is that Z = 5.7 for <u>both</u> days. Then undoubtedly the spot observed on July 7 is brighter at 5893.4Å than the spot observed on Feb. 28. In fact, now the continuum of the spot at 5893.4Å is in good agreement with the continuum predicted by the model of Kneer (1972) (see Figure 1). This same model also predicts an intensity between the D lines close to that observed (see Figure 3). Again assuming Z = 5.7, we find that the maximum intensity between the sodium D lines is 0.585. The error bars extend to 0.647 (with Z = 4.3) and 0.448 (with Z = 7.75). Figure 3 indicates that these results are in quite good agreement with those determined on Feb. 28. Taking both continuum and line

intensities into account, our observations suggest that Kneer's model provides the best overall fit to the observations.

c. Photoelectric Magnetometer Observations

On July 6, 1973, the magnetometer was used to observe polarization in the sodium D_2 line in a sunspot (A_u = 60). To obtain large photon counting rates, both entrance and exit pinholes were opened up to 0.4 mm. This corresponds to an exit window of 1.2Å. The large apertures drove the counters to saturation when observing the photosphere. Scattered light at one arc minute from the limb was 2×10^5 c/sec. Assuming that this represented 1.11% of central disk intensity (as recorded in the narrow channel on July 7), the latter must have been 1.81×10^7 c/sec. In the spot, count rates were in the range $(2.5 - 2.9) \times 10^6$ c/sec. Assuming a Zwaan factor of 5.7 for the narrow-band data, the scattered light to be subtracted from spot counts is 1.14×10^6 c/sec.

The counting rates in the difference channel (i.e. difference between left and right circularly polarized components) were +6130, +5600, -5420, -1080, and +1740 c/sec at distances from the line center of $\Delta\lambda$ = -1.5, -1.0, +1.0, +1.5, and +2.0 Å respectively. The r.m.s. deviations from these mean values were respectively $\pm$1250, $\pm$1350, $\pm$2990, $\pm$2120, and $\pm$1860 c/sec. Thus the first two counts, and probably also the

third, represent positive detection of circular polarization in the D_2 line, with a degree of polarization up to 0.4%. Figure 4 shows the results. In plotting the polarizations in the spot, zero point shifts of order 0.01 - 0.03% have been removed by monitoring the photosphere, where it is assumed that the true polarization is precisely zero. Figure 4 suggests that there is indeed a change of sign of polarization in traversing the line center. More observations are needed near the line center, but clouds prevented continuation of the observations on July 6.

The curve in Figure 4 is <u>not</u> meant to be a fit to the observed points. It is a smoothed version of the polarization curve predicted by Yun (1972) for a field of 2400 gauss viewed along the field lines, <u>but with all theoretical polarizations reduced by a factor of 10</u>. The method of smoothing was as follows. Values of Δ (the difference in % between left and right polarization) were read off Yun's predicted curve (Figure 10 of Yun, 1972) at intervals of 0.1Å. Yun's curve does not approach the line center any closer than 0.6Å, for non-LTE effects are probably essential in the core of the line. It is known, however, that Δ must go to zero at line center, so we adopted the simple expedient of joining the termination of Yun's curve to the origin by a straight line. From Figure 9 of Yun (1972) relative intensities in the line were read off at 0.1Å intervals. Again, the line profile had not been computed by

Yun within 0.6Å of the line center, but it is known that the central intensity of the D_2 line in a spot is between 3 and 4% (Fay, Remo, and Czaja, 1972). We therefore drew a straight line between the last point on Yun's profile and 4% relative intensity at line center. Then the smoothed polarization was determined from

$$\bar{p} = \sum_{i=-6}^{+6} \Delta_i I_i \Big/ \sum_{i=-6}^{+6} I_i$$

where the summations extend over all points within a 1.2Å band centered on $\Delta\lambda$. The results are as follows.

$\Delta\lambda$(Å)	0	0.5	1.0	1.5	2.0
$\bar{p}$	0	2.69%	2.20%	1.25%	0.73%

By reversing the sign of p on opposite sides of line center we have obtained the smoothed curve in Figure 3. But it must be remembered again that in drawing the curve, we have reduced all polarizations by a factor of 10.

The observed polarizations are much smaller than those predicted by Yun. Moreover, the observed polarizations do not seem to be symmetric about line center. A similar effect is indicated by the photographic observations of Baranovsky and Stepanov (1959). These problems may be due to the use of large pinholes. Using a more sensitive photomultiplier (EMI 9502S) we observed the NaD_2 line in a small spot (A_u = 30) on Aug. 30, 1973 using entrance and exit pinholes of 0.1 mm, corresponding

to wavelength resolution of $\pm$0.15Å. Results are in Figure 5. The error bars are large because counting rates are low near the line center. But the mean values do reach $\pm$6% on opposite sides of the line center, in accordance with Yun's prediction, though the location of 6% polarization is considerably closer to the line center than Yun's prediction. This may indicate fields weaker than the 2400-3000 gauss fields used by Yun, or may indicate that the field is not exactly along the line of sight (as assumed by Yun). Clearly, the sign of $p_R - p_L$ at positive $\Delta\lambda$ in Figures 4 and 5 indicate that the spots of July 7, 1973 and Aug. 30, 1973 were of opposite polarity.

d) Umbral Scattered Light Corrections

Earlier analyses of Zwaan (1965) and Staveland (1970) have been extended in two ways. One is to extend the series describing the limb darkening of the solar disk; the second is to obtain an analytic solution for a Gaussian scattering function. The limb darkening series has been extended to include terms up to $\sin^{12}\alpha$ (α being the angle between the normal to the solar surface and the line of sight). Previous series have terminated at either $\sin^4\alpha$ or $\sin^6\alpha$. More exact representation of the solar disk intensity near the limb is now possible, with the result that the aureole intensity computed near the limb may be appreciably different from that obtained using a lower order approximation to the limb darkening. The differences

are especially obvious when one deals with Gaussian scattering functions very close to the limb. Thus the parameters one derives to describe the observed aureole are different when one uses different orders of approximation in the limb darkening series. This means that extrapolation of the aureole on to the disk leads to different values of scattered light on the disk. For a discussion of the influence of observational errors see end of Section Ia.

Previously published work (by Wöhl et.al.(1970), Mattig (1971), etc.) has not included analytic expressions for the aureole in the case that the scattering functions are Gaussian. If the limb darkening can be expressed as a series in $\sin^2\alpha$ (as for the Lorentzian scattering functions), it is possible to obtain recursion relations for the coefficients in a series expression for the aureole. The solution is made possible by using one of the definitions of the modified Bessel functions of zero order, as well as a standard integral over the product of two Bessel functions. The solution divides into two parts, one on the disk, far from the limb, and the second in the aureole, again far from the limb. The transition region is described to a high order of approximation by a hyperbolic tangent function, as this function has the advantage of the correct asymptotic form at disk center (where an exact solution is available).

Theoretical aureoles have been computed to fit observa-

tions made at Bartol on October 30, 1972, and to fit results published by Mattig (1971). The procedure is to express all observed and computed intensities in terms of the intensity at one point, at a distance of one arc minute from the limb, and then the scaling factor is provided by fitting to the observed absolute intensity at that point. It has been found that the set of parameters describing the aureole is not unique. In particular, the parameter B describing the half-width of one of the Lorentzian scattering functions can be made arbitrarily small (below a certain upper limit) without affecting the computed aureole by more than a small fraction of one percent. Aureole observations at Bartol are accurate to better than 0.5% (other observatories do not have as high accuracy as this), but even this accuracy is not sufficient to distinguish between an infinite series of theoretical aureoles. Unfortunately, the smaller B is, the larger the scattered light extrapolated on to the disk becomes, and we are faced with a logarithmic divergence on the disk.

The resolution of this dilemma <u>should</u> be provided by proper normalization of the scattering function. But here we encounter the main difficulty of using a Lorentzian scattering function —— the normalization integral also diverges. Following Zwaan, it has been traditional to limit the range of integration to a distance of 90 degrees from the sun, but we have found

that in order to fit Mattig's observed aureole by this condition, we must choose $B = 2 \times 10^{-39}$. The scattered light on the disk then becomes unreasonably large, 23% of disk center intensity.

Instead, we may say that there is an absolute upper limit to the scattered light on the disk provided by (i) observations at Bartol sunspot intensity (before correcting for scattered light), and (ii) Mattig's observations of Mercury during transit across the solar disk. Scattered light cannot exceed the observed intensities in both cases, and the observed values turn out to be 7.8 and 7.7 times the intensity observed in the aureole at a distance of one arc minute from the limb. (The agreement in numbers is probably fortuitous.) These numbers set a lower limit on B, which in turn sets a lower limit on the integration limits of the normalization integral. Instead of 90 degrees, as proposed by Zwaan, the lower limit turns out to be greater than this by a factor of almost 10^6. Clearly, the use of Lorentzian scattering functions is the weakest part of aureole theory.

III. Theoretical Work at the Bartol Observatory

a) Umbral Model Atmospheres

About two years ago we proposed a new model atmosphere of a medium-to-large sized umbra based on our photoelectric observations of Na I D_2 line profiles. We have shown that the proposed model not only accounts for the continuum observations

available at that time (e.g. Wittmann and Schröter (1969)), but also for some other major Fraunhofer line profiles.

According to most recent continuum observations (see Figure 6) by Mattig (1971), Kneer (1972) and Stellmacher and Wiehr (1972), including our own observations by Mullan and Wyller (1972), the observed umbral continuous intensities are consistently lower than those of the earlier observations made by Wittmann and Schröter by a factor of nearly two. This gives rise to a serious reexamination of our earlier proposed model. Since our proposed model describes the observed Na I D_2 profiles fairly well, a new umbral model has to be constructed in such a way that the resulting temperature distribution should not influence appreciably the line profiles.

During the research period such attempts have been made and the results are presented in Figures 1, 3, and 6, where YWI and YWII represent our newly adopted models. In these figures, other leading umbral models have been included by denoting KN for Kneer's model, SW for Stellmacher and Wiehr and YW for our earlier model. As noted from Figures 1 and 6, our new umbral models, YWI and YWII differ from the earlier model, YW in temperature, which has been reduced by 300 to 500 K, just enough to make an account of the new observed ratios of the umbral-to-disk continuum intensities. YWI and YWII, in general, are quite similar to each other except for the deeper region, $\tau_{5000} > 1$

where a temperature difference of 100 to 300 K exists due to some minor adjustment made to the temperature distribution in order to describe the observed profiles of Na I D_2 and Fe 5435 lines respectively.

From the continuum observations alone it is difficult to assess the new models YWI and YWII. It appears evident that the temperature distribution in the upper layers in leading umbral models are in good agreement with each other as demonstrated in Figure 6. However, when additional information on the continuum depression between the line wings of Na D_1 and D_2 is taken into account (see Figure 3) it would appear that Kneer's model provides the overall best fit to the observations both in the continuum and the Na D line wings. The final outcome rests solely on the precision with which the contributions from scattered light by the aureole can be removed. As seen from Figure 3, the corrected observations would favor the model YWI if Z = 4.3 and SW if Z = 7.75, but then in neither case would the continuum observations be consistent with the models. Coronagraph observations or observations in space are obviously essential to resolve this question (see section Id).

b) Umbral Flashes and Running Penumbral Waves

During the course of this research period we have successfully incorporated Öpik's theory of convection (1950) into our

computer program of sunspot models. Because of its essential feature of the ability of taking care of the occurrence of transverse motion as well as the vertical gas flow, the present program is especially well suited for studying the effect of magnetic fields on convective cells in sunspots, when a spread function f_m (which describes the horizontal motion of the gas across the field line) is properly evaluated.

Early this year, it has been noted by Moore (1972) at the Big Bear Solar Observatory that umbral flashes and running penumbral waves in sunspots (Zirin and Stein, 1972) may be attributed to a manifestation of overstable oscillations generated beneath the visible layers of the umbrae. His analysis, however, critically depended on the assumption that the growth time of the oscillation τ_e must be much shorter than the rate of dissipation τ_D and also on the numerical values of the seven parameters to be specified at each depth for the evaluation of the growth time and the rate of dissipation (i.e., density, scale height, thermal expansion coefficient, superadiabatic temperature gradient, electrical conductivity σ, thermal diffusivity and magnetic field strength). Some of these quantities vary by orders of magnitude as functions of depth in the upper few hundred km of the spot. Noting that in his analysis, Moore has relied on the numerical values of the relevant seven parameters only at <u>two</u> particular depths and that he has employed the fully ionized electrical conductivity

given by Spitzer (1962), we have taken Moore's analysis as worthy of further investigation by reexamining the depth-dependence of τ_e and τ_D in our recently computed spot model based on a more accurate expression for the electrical conductivity by Wyller and Yun (1972). In our analysis, local values of all seven parameters are used to estimate the growth time and the rate of dissipation. In computing sunspot model the surface magnetic field is taken to be 3000 gauss at the surface ($\tau = 2/3$) with a vertical gradient of 0.7 gauss/km. Among various effective temperatures of spots, we have adopted $T_e = 3300^{\circ}K$, since this leads to a spot model having a convection zone equal in depth to the depth of the solar convection zone as computed by Mullan (1971).

A notable feature of our calculations is the large increase in η=magnetic diffusivity in the surface layers when partial ionization is allowed for. This causes a proportional decrease in Joule dissipation time. In order to examine how sensitive Moore's conclusions are to the choice of σ, we have computed two models with $T_e = 3300$ K: one makes use of the accurate conductivity, while the other uses the fully ionized conductivity given by Spitzer (1962). Moore's analysis of overstable oscillations is then applied to both models, leading to the results in Figure 7 (accurate σ) and Figure 8 (Spitzer's σ). These figures show growth times and periods of oscillations, as well as Joule dissipation times, as functions of depth. The shape of a convection cell varies with

depth, and the local values of the shape parameter, s, are indicated where s is defined by Moore, and here taken to be equal to the ratio of cell diameter to cell depth D/H. There are marked differences between the two models, especially in the surface layers. Even in the deeper layers where ionization is essentially complete, there are still differences between the two models. These are due to changes in the structure of the model arising from the effects of electrical conductivity in the magnetic spreading parameter f_m. Physically, the effect is that higher conductivity restricts horizontal cell size, thereby reducing the efficiency of convection.

As seen in Figure 6, our refinement of Moore's analysis substantiates his mechanism for the generation of umbral flashes and running penumbral waves in sunspots. However, because of significant differences in our results arising from whether the conductivity is taken to be that of a fully ionized gas or that of a partially ionized gas in a magnetic field, in particular its pronounced differences in the surface layers, it is found that contrary to Moore's conclusion, oscillations cannot grow within 250 km of the surface. The source of oscillations must lie deeper than 250 km, though not as deep as 650 km, where Moore suggests penumbral waves are generated (see Figure 6). Our results lead us to believe that both umbral flashes and penumbral waves could be excited in essentially the same region, from

300 to 400 km beneath the surface.

c) Sunspot Interior Models with Alfvén Wave Emission

There have been two general approaches in the computation of sunspot models. The first assumes that the thermal flux of energy is constant at all depths, and is equal to the flux observed at the surface of the spot. This is the approach used by Deinzer (1965), Yun (1970), Lykoudis (1971) and Mullan (1973). The second approach attempts to describe how the thermal flux varies with depth, for it is argued that ultimately the flux must increase from the low surface value to the flux which emerges from the deep interior of the sun (cf. Chitre, 1963; Chitre and Shaviv, 1967). Of the two approaches, the second is physically more realistic, but Chitre and Shaviv could not exploit this physical advantage to the full on account of a deficiency in the convection model which they used. Their convection model (a mixing-length model) did not include any feature which would allow them to estimate how large the thermal flux should be at any particular depth. Because of this, a certain degree of arbitrariness was inevitable, and they realized that their solution was not unique.

In our present work, we adopt the second approach, and the arbitrariness of the solution is essentially removed by using a convection model which overcomes the deficiency encountered by

Chitre and Shaviv. Our model differs from the mixing-length model in that convection occurs in cells, where part of the gas motions are horizontal. The interaction between these horizontal motions and the vertical field lines creates Alfvén waves, and our model allows us to estimate the flux of Alfvén waves at any depth from considerations of the horizontal size of the cells at that depth. We can then compute the thermal flux at each depth uniquely if we assume that the sum of the Alfvén wave flux and the thermal flux (radiative plus convective) remains constant at all depths, and is equal to the flux emerging from the solar interior, 6.33×10^{10} ergs cm^{-2} sec^{-1}.

The uniqueness of our solution depends on the assumption that all of the missing flux in a spot is carried by Alfvén waves. The reason for limiting our attention to Alfvén waves alone is not merely because these are the waves with the simplest physical properties. Considerations of expected fluxes and of dissipation are also important. We expect that the flux of magnetosonic waves would not exceed the flux of the equivalent wave mode generated by convection in non-magnetic regions — sound waves. If the chromosphere is heated by sound wave dissipation (Osterbrock, 1961), the energy flux in the waves is of the order of 10^7 ergs cm^{-2} sec^{-1}, i.e. less than 1% of the thermal flux emerging from a spot. The flux of magnetosonic waves in a spot might be even smaller than the sound wave flux in non-magnetic regions, on

account of the reduction of convective efficiency in the spot. But even if this is not true, it seems to be a good approximation to neglect magnetosonic waves in a spot. We also expect that, as far as wave dissipation is concerned, magnetosonic waves are subject to dissipative processes which have no effect on Alfvén waves (to first order in wave amplitude; cf. Chin and Wentzel, 1972). Other things being equal, then, magnetosonic waves dissipate more rapidly than Alfvén waves. Dissipation has the effect of returning energy to the thermal content of the gas in the spot, and so from an overall point of view, energy converted into magnetosonic waves is not really lost from the thermal flux. On the other hand, once convective energy has been converted into Alfvén waves, we assume that this energy is irretrievably lost from the thermal flux. The assumption of negligible damping of Alfvén waves seems to be a good approximation, for damping lengths in solar conditions are 10^8 km (Osterbrock, 1961; assuming B = 3000 gauss, and wave periods of a few hundred sec). There is of course always the possibility that physical conditions might change locally so as to permit rapid dissipation of Alfvén waves, but in this work we assume that dissipation of Alfvén waves is unimportant.

Sunspot models have been computed with the assumption that the missing flux is transported by undissipated Alfvén waves. In order to estimate the flux of these waves, we extend Öpik's (1950)

cellular model of convection to include the effects of a vertical magnetic field. Öpik's model is very well suited to the present work, for it includes horizontal gas motions, and it is these motions which both are influenced by and influence the field. Horizontal motions, not vertical motions, are impeded more or less severely depending on the electrical conductivity, and this reduces the convective flux. These motions, however, shake the field lines, and this is assumed to be a source of Alfvén waves, compensating for the reduction in the convective flux. In Figure 9, the initially vertical field line AA' is distorted by cellular motion into a square wave shape. In order to estimate the horizontal field strength B_h, the square wave is replaced by a triangular wave, which is related to the square wave by vector addition. Then B_h is related to the total field B by a simple function of D/H. The component B_h is here assumed to be the amplitude of an Alfvén wave, and the flux of Alfvén waves can therefore by expressed in terms of D/H, to within a numerical factor ϵ. The free parameter D/H (ratio of cell diameter to cell depth) is adjusted such that the total sum of radiative, convective, and Alfvén wave fluxes remains constant at all depths and equals the undisturbed solar flux entering the spot from below.

We derive the depth-dependence of the three fluxes (see Figure 10) and of the effective temperature T_e in a spot, and find that T_e increases non-monotonically from a low value at the sur-

face (2750 K in a spot with magnetic field B = 3000 gauss) to the solar value (5780 K) at depth Z (see Figure 11). The latter turns out to lie within 1% of the depth of the solar convection zone in all cases of interest. Convection cells in sunspots are found to be narrow cylinders ($D/H \lesssim 0.2$) aligned along the field lines, in accordance with physical expectations. The diameter of a cell at the top of a spot with B = 3000 gauss, is of the order of 80 km, which is an order of magnitude smaller than the diameters of photospheric convection cells. Cell diameters decrease at larger field strengths. The depth z_A where the Alfvén wave flux has a maximum is found to be 841 km in a spot with B = 3000 gauss, and z_A decreases with decreasing B. The values of z_A seem to correspond with the "Wilson depression". Radiative influx of heat from the walls of a spot is found to be minimal for B = 2000-3000 gauss, and increases rapidly outside this range (see Figure 12). Thus spots with B in this range are expected to live longest, and the most common observed field strengths are expected to lie in this range. If radiative heating is responsible for the lower limit on the permissible field strength in spots (1200 gauss), then there should also be an upper limit on spot field strength at 5300 gauss. This agrees with observations of Steshenko (1967) who found the maximum observed field strength in a spot to be 5350 gauss.

The effective temperatures are lower by 10^3 K than observers usually quote for sunspots. However, the numerical values of T_e are sensitive to an efficiency factor ϵ in the expression for the flux of Alfvén waves. The value T_e = 2750 K for B = 3000 gauss is definitely a lower limit on T_e, and if the ϵ is increased by a factor 2 (which is not unreasonable), T_e rises to 3000 K. In view of the great uncertainties in scattered light corrections (see Section Id above) it is not out of the range of possibility that sunspot effective temperatures will continue to become lower and lower with improved observational techniques. In 1965, for example, Bray and Loughhead (1965) quoted effective temperatures of spots as high as 4160-4480°K, with a temperature difference between spot and photosphere of 1625K, at the level of the atmosphere where $T = T_e$. In 1968, Kneer and Mattig (1968) made careful corrections for scattered light and found that the temperature difference between spot and photosphere at $\tau = 1$ is 2700 K. This refers to a slightly deeper layer in the atmosphere than that referred to by Bray and Loughhead, but nevertheless, the sunspot intensities deduced by Kneer and Mattig are unmistakably darker than those considered three years previously by Bray and Loughhead. At least part of the difference arises from careful attention to reducing scattered light in the observations, and careful attention to correcting for what scattered light <u>is</u> present. If this trend continues,

the "true" effective temperatures of sunspots may turn out to be as cool as 3000 K. Indeed, 3300 K seems to be the best current value if umbral flashes and penumbral running waves are to be explained in terms of hydromagnetic overstability (Mullan and Yun, 1973).

One result of the work with Alfvén waves in spots has been to suggest that purely radiative models of sunspots may not after all be permissible. This conclusion is based on our simple model of Alfvén wave generation, for if no convection occurs, then no Alfvén waves can be generated according to our model. Then there would be no reason for flux to be missing, for thermal flux transported by convection can be simply transported by radiation if convection is suppressed. The temperature gradient would need to be steeper, and this would lead to a lower surface temperature, but effective temperature would not necessarily change, and a spot would not appear dark. There might however be plasma instabilities of a kind totally different from the simple physical mechanism we have considered. In that case, Alfvén waves might be generated even in an entirely radiative spot, and our earlier models (Mullan, 1973) might still be valid.

d) Miscellaneous

1. Convection Rolls in Penumbrae

Danielson (1961) suggested that penumbral filaments might be convection rolls oriented along the magnetic field lines. Beckers and Schröter (1969) thought they had confirmed this suggestion when they observed the bright filaments (BF) to be rising relative to the dark filaments (DF). However, they also claimed to have seen stronger magnetic fields in DF than in BF. Stronger fields in DF should contribute to buoyancy of the DF relative to BF, and should therefore tend to make the DF rise relative to BF, rather than the reverse. If BF do in fact rise relative to DF, then the gas density in BF must be less than that in DF at equal geometric depths. Assuming that there is pressure equilibrium one can then derive an upper limit on the permissible excess of magnetic field strength in DF relative to BF. The permissible excess turns out to be very small, less than 2% of the mean penumbral field. Observations suggest (though not definitively) that the excess field in DF is probably greater than 2% of the mean field. The observations are therefore inconsistent, and cannot be taken as proof for the existence of convection rolls in penumbral filaments.

2. Radiative Sunspot Model

Convection is generally assumed to be inhibited in a spot as a result of the magnetic field. However, if convection

is completely suppressed, radiation might be expected to carry all of the flux emerging at the surface. Chitre (1963) showed that this would lead to great difficulties if one uses a model for the solar convection zone based on the mixing-length theory of convection. The latter leads to high densities and pressures in the convection zone, and a sunspot penetrating into the convection zone would require extremely high fields (1.4×10^5 gauss) to be in magnetohydrostatic equilibrium. And even if this (horizontal) equilibrium were achieved, the gas in the spot would be an order of magnitude less dense than the gas in the surrounding convection zone at equal depth. The gas in the spot would then be violently unstable with respect to vertical displacements.

These difficulties are largely overcome if one uses a model of the solar convection zone based on Öpik's cellular convection theory (Öpik 1950). In this model, pressures and densities are lower than in the mixing-length model, with the result that it is possible to compute a perfectly acceptable spot model in both radiative and magnetohydrostatic equilibrium. The field gradient nowhere exceeds 1 g/km, the field at the base of the spot is only 9×10^3 gauss, and the density in the spot at the base is equal to the density of the gas in the convection zone at the same depth. Within the framework of the model, the condition of equal densities inside and outside the spot at the base of the convection zone leads to the conclusion that there is a

unique effective temperature for all spots, namely, 3800°K.

3. Sunspots and the Depth of the Convection Zone

One of the principal results to emerge from an application of Öpik's convection model to the sun was that the depth of the convection zone was very small, close to 10^4 km (Mullan, 1971). It was suggested that supergranules were convective cells of some kind penetrating through the entire zone, with diameter to depth ratios D/H of about 3. The latter is the value typical of convection cells in laboratory conditions, and D/H $\approx$ 4 seems to be the typical value for small-scale convection cells in the sun, namely, the solar granules. Our results on Alfvén wave models (see above) suggest that sunspots penetrate through the entire convection zone also, so their diameters on the surface are expected to be related to the depth of the convection zone by simple D/H values. Theoretical values expected for D/H are given by Vickers (1971) and they suggest that surface diameters of convection cells penetrating through the convection zone should lie in the 18-65 thousand km.

Bumba et al. (1973) have observed that sunspot diameters are quantized, or at least favor certain preferred values. The preferred values are 19, 27, 35, 46 and 54 thousand km. These seem to lie within the limits we expect from a convection zone of depth 10^4 km.

A further argument for a shallow convection zone is provided indirectly from measurements of the velocity of upward motion of magnetic flux ropes breaking through the surface to form sunspots. The upward velocity is 115 $\pm$ 30 meters/second (Vitinsky and Ikhsanov, 1966) independent of sunspot area. Now a rising flux rope gives warning of its impending arrival by producing changes in the photosphere. Thus, photospheric and chromospheric faculae appear, granules brighten and become aligned, gas motions in the photosphere are set up in such a way as to flow down a magnetic hill beginning to push its way up to the surface (Vassilyeva et al., 1971). The earliest warning of the flux tube occurs 2-3 days before a sunspot appears. We can interpret these facts by a simple model. Suppose a flux tube is buoyed upwards from the deep interior towards the surface. Then as long as the flux tube is in a radiative region, the tube should not emit any Alfvén waves and the tube has no way to communicate to the surface layers that it is coming. Now let it come into contact with the bottom of the convection zone. Waves are created when the convective gas motions shake the flux tube. It is these waves which propagate to the surface (we surmise) and warn the surface that the flux tube is coming. Let the buoyant acceleration of the flux tube be α inside the convection zone. In the time T taken for the flux tube to rise from the bottom of the convection zone to the surface, the

upward velocity v is given by $v = u + \alpha T$ where u is the initial upward velocity of the flux tube when it encountered the deepest part of the convection zone. The maximum value of α is obtained by assuming u = 0. Then $\alpha = v/T = 1.15 \times 10^4/2 \times 10^5 = 0.05\text{-}0.06$ cm/sec^2, where we have inserted the velocity observed for flux tube rising, and T = 2.3 days. The depth of the bottom of the convection zone then follows as $s = \frac{1}{2} \alpha T^2 = \frac{1}{2} vT \approx 10^4$ km.

4. Triggering of Solar Flares Near Sunspots

Wolff (1972a,b) has suggested that free modes of oscillation of the sun can be energized by superadiabatic temperature gradients. According to our sunspot models, a sunspot is a place where the efficiency of convection is reduced and in order to carry a certain flux of radiative and convective energies, the temperature gradient must steepen. Around a sunspot, in a plage region, the same phenomenon is expected to occur although the field strengths are not necessarily large enough to cause a sunspot to form. The principal characteristic of a plage is then its larger than normal superadiabaticity. According to Wolff, then, a plage should be a favorable location for observing free modes of oscillation of the sun. The signature of such modes is large scale coherence in the gas motions.

Coherent gas motions on scales of 60-110 thousand km have been observed in plages by Tanaka (1972) in the light of $H\alpha$. We suggest these are evidence for free modes of the sun.

Coherence makes for large fluxes of mechanical energy, and we have estimated (Mullan, 1973b) that the oscillations observed by Tanaka can transmit up to 10^{34} ergs to the chromosphere during their lifetimes. Such enormous energies are more than sufficient (by factors of 100) to account for even the largest solar flares, and we suggest that the coherent oscillations may at least trigger flares, if not in fact provide all of the energy released as well. Tanaka's most important result was indeed that coherent oscillations were the predecessors of flares.

IV. Personnel Activities

Paper Presentations and Meeting Attendance

1. "Seven colour Photometry of Umbral Cores with the Bartol Coudé Telescope" by D.J. Mullan and A.A. Wyller. Paper presented at the 139th Meeting of the American Astronomical Society in Las Cruces, New Mexico. January 9-12, 1973.
2. "The Behaviour of HeI λ5876 and λ10,830 over Sunspot Umbrae" by A.A. Wyller and D.J. Mullan. Presented at the OSO-I Guest Investigator Meeting held in Paris. March 5-8, 1973.
3. Attendance by D.J. Mullan at 140th Meeting of American Astronomical Society, Columbus, Ohio, June 25-28, 1973.
4. Attendance by A.A. Wyller as member of Commissions 12, 29 and 36 at the 15th General Assembly of the International Astronomical Union, in Sydney, Australia, August 20-31, 1973.

Papers Published

1. "Are Penumbral Filaments Convection Rolls?" by D.J. Mullan, Astronomy and Astrophysics 24, 103, 1973.
2. "Seven Color Photometry of Umbral Cores with the Bartol Coudé Telescope", by D.J. Mullan and A.A. Wyller, Bulletin of the American Astronomical Society 5, 20, 1973.
3. "On the Possibility of Constructing a Radiative Sunspot Model in Magnetohydrostatic Equilibrium", by D.J. Mullan, Solar Physics 30, 75, 1973.
4. "Can Oscillations Grow in a Sunspot Umbra?" by D.J. Mullan and H.S. Yun, Solar Phys. 30, 83, 1973.
5. "Earthquake Waves and the Geomagnetic Dynamo" by D.J. Mullan, Science 181, 553, 1973.

Papers in press

1. "Flare Triggering by Coherent Oscillations" by D.J. Mullan, Astrophysical Journal, Vol. 185 (Oct. 1, 1973 issue, in press).
2. "Sunspots, Supergranules, and the Depth of the Solar Convection Zone" by D.J. Mullan, Astrophysical Journal Vol. 186 (Dec. 15, 1973 issue, in press).
3. "Sunspot Models with Alfven Wave Emission" by D.J. Mullan, Astrophysical Journal, Vol. 187 (Feb. 1, 1974 issue, in press).
4. "Correction of Sunspot Intensities to Scattered Light" by D.J. Mullan, Solar Physics (in press).

5. "Comments on Papers by P.R. Wilson Concerning Sunspots" by D.J. Mullan, Solar Physics (in press).

6. "Fast Rotation of Metal-Poor Stars" by D.J. Mullan, 1973, Astronomy and Astrophysics (in press).

7. "URSIES and the Bartol Coudé Observatory" by A.A. Wyller, Proceedings of the First European Astronomical Meeting, Vol. 2, 1973.

Personnel Changes

During the past year Dr. Yun resigned to take up a position as Professor at Seoul National University in South Korea. Dr. Wyller changed to a part-time basis, while taking up responsibilities as Research Professor and Director of the Swedish Astrophysical Observatory at Anacapri, Italy, under the auspices of the Royal Swedish Academy of Science.

Dr. Mullan continues full-time work on the project and Dr. Hegyi, from the Smithsonian Astrophysical Observatory, has recently joined the Bartol staff. While Dr. Mullan will concentrate his efforts mainly on theoretical work (taking over some of Dr. Yun's programs), Dr. Hegyi will be mainly responsible for the day to day running of the solar telescope at Bartol.

V. References

Baranovsky, E.A. and Stepanov, V.E., 1959, Izv. Krim. Astrophys. Obs. 21, 180.

Beckers, J.M., Schröter, E.H., 1969, Solar Physics 10, 384.

Bray, R.J. and Loughhead, R.E. 1965, Sunspots (Wiley, New York).

Bumba, V, Ranzinger, P, Suda, J., 1973, Bull. Astron. Inst. Czechoslovakia 24, 22.

Chin, Y.-C. and Wentzel, D.G., 1972, Astrophys. Space Sci. 16, 465.

Chitre, S.M., 1963, Monthly Notices Roy. Astron Soc. 126, 431.

Chitre, S.M. and Shaviv, G., 1967, Solar Physics 2, 150.

Danielson, R.E., 1961, Ap. J. 134, 289.

Deinzer, W., 1965, Astrophys. J. 141, 548.

Fay, T.D., Remo, J., and Czaja, K., 1972, Solar Physics 26, 87.

Henoux, J.C., 1969, Astron. and Astrophys. 2, 288.

Kneer, F., 1972, Astron. and Astrophys. 18, 39.

Kneer, F. and Mattig, W., 1968, Solar Phys. 5, 45.

Lykoudis, P., 1971, Bull. Am. Astron. Soc. 3, 461; also preprint May 1972.

Mattig, W., 1971, Solar Physics 18, 439.

Milford, N., 1950, Annales d'Astrophysique 13, 243.

Moore, R.L., 1972, "On the generation of umbral flashes and running penumbral waves", Big Bear Solar Observatory #0126.

Mullan, D.J., 1971, Monthly Notices Roy. Astron. Soc. 154, 467.

Mullan, D.J., 1973a, Solar Physics 30, 75.

Mullan, D.J., 1973b, "Flare Triggering by Coherent Oscillations", Astrophys. J. 185 (to appear in Oct. 1 issue).

Mullan, D.J. and Yun, H.S., 1973, Solar Physics 30, 83.

Mullan, D.J. and Wyller, A.A. 1973, Bull. Amer. Astron. Soc. 5, 20.

Öpik, E.J., 1950, Monthly Notices Roy. Astron. Soc. 110, 559.

Osterbrock, D.E., 1961, Astrophys. J. 134, 347.

Spitzer, L., 1962, Physics of Fully Ionized Gases, Interscience, New York, 2nd edition, p. 143.

Staveland, L., 1970, Solar Physics 12, 328; also Report No. 36, Inst. Theor. Astrophys., Oslo, 1972.

Stellmacher, G. and Wiehr, E., 1972, Astron. and Astrophys. 19, 293.

Steshenko, N.V., 1967, Izvestia Krimskoi Astro. Observ. 37, 21.

Stumpff, P., 1961, Zeitschr. f. Astrophys. 51, 73.

Tanaka, K., 1972, "Chromospheric Oscillations in Hα Plage", Big Bear Solar Observatory preprint.

Vassilyeva, G.Y., Korobova, Z.B. and Chandaev, A.K., Izvestia Pulkovo Observ. No. 186, p. 19.

Vickers, G.T., 1971, Astrophys. J. 163, 363.

Vitinsky, Y.I. and Ikhsanov, R.N., 1966, Izvestia Pulkovo Observ. No. 180, p. 20.

Wittmann, A. and Schröter, E.H., 1969, Solar Physics 10, 357.

Wöhl, H., 1970, Solar Physics 15, 338.

Wöhl, H., Wittmann, A., Schröter, E.H., 1970, Solar Physics 13, 104.

Wolff, C.L., 1972a, Astrophys. J. 176, 833.

Wolff, C.L., 1972b, Astrophys. J. Letters 177, L87.

Wyller, A.A. and Yun, H.S., 1972, Solar Physics 21, 116.

Yun, H.S., 1970, Astrophys. J. 162, 975.

Yun, H.S., 1971, Solar Physics 16, 379.

Yun, H.S., 1972, Semi-annual report submitted to NASA, March 9, 1972.

Zirin, H. and Stein, A., 1972, Astrophys. J. Letters 178, L85.

Zwaan, C., 1965, Rech. Astron. Obs., Utrecht XVII, No. 4

Captions for Figures

Figure 1. Umbra to disk intensity as functions of wavelength. Observations of Mattig, of Kneer, of Mullan and Wyller, and of Mullan are plotted. The kinked solid and dashed lines are composed of straight-line segments drawn between broad-band observations of Mullan and Wyller. The monotonic solid lines are theoretical continuum intensity ratios predicted by the models of Stellmacher and Wiehr (SW), Kneer (KN) and various models of Yun.

Figure 2. Aureole observed in broad band (λ = 4900 Å) on July 6, 1973 is indicated by open circles. The theoretical curve is derived from the scattering function indicated. Error bars on the aureole intensities are less than 1%. More important may be the horizontal error bars, particularly on the point closest to the disk, at R/R_o = 1.0175 (see text).

Figure 3. Overlapping wings of the sodium D lines. $\Delta\lambda$ is measured from the center of the D_2 line at 5890Å. Theoretical wing profiles are computed from the models used in Figure 1. Observations at Bartol Observatory on Feb. 28, 1973 are shown. The Zwaan factor Z for the scattered light correction has a best value of 5.7 (point B). Error bar C corresponds to the maximum permissible Z, and C is a firm lower limit on I_λ/I_c. Error bar A corresponds to the minimum Z compatible with the errors in aureole determination.

Figure 4. Δ is the difference between left and right polarizations in the wings of the sodium D_2 line, expressed as a percentage of total light intensity observed. The observations refer to a spot observed July 6, 1973. The error bars are r.m.s. deviations in the counting rates. The curve is a scaled down version (reduced by a factor of 10) of the theoretical polarization computed by Yun (1972), and smoothed over a range of wavelengths $\pm$ 0.6 Å on either side of $\Delta\lambda$. The observed polarizations are much smaller than the theoretical predictions. Large entrance and exit apertures have to be used in order to achieve significant statistics.

Figure 5. Same as Figure 4 for spot observed Aug. 30, 1973, A_u = 30. Entrance and exit pinholes 100 microns, corresponding to wavelength range $\pm$ 0.15 Å on each side of $\Delta\lambda$. Observed polarization increase to 6%, as predicted by Yun, but the small pinholes make for poor statistics.

Figure 6. $T = \tau_{5000}$ relations of our new empirical umbral models, YWI and YWII. Other leading models are designated by YW = Yun (1971), SW = Stellmacher and Wiehr (1972) and KN = Kneer (1972).

Figure 7. Computed growth time, τ_e, magnetic diffusion time τ_D, and period of oscillation in the umbral model of $T_e = 3300^oK$ by making use of the accurate electrical conductivity. s is the shape factor defined as the ratio of vertical to horizontal size of a convective cell, H/D.

Figure 8. Computed τ_e, τ_D and period of oscillation in the umbral model of $T_e = 3300^oK$ by using the fully ionized electrical conductivity given by Spitzer (1962).

Figure 9. In order to estimate the amplitude of Alfven waves generated by convective gas motions, we imagine an initially vertical field line AA' (Fig. 9(a)). Cellular motion distorts this field line into a square

shape (Fig. 9(b)). In Fig. 9(c), vectors PN and QP are vector sums of GF + FE and KJ + JG in Fig. 9(b). By replacing the square in (b) by the vector equivalent triangle in (c) we can estimate the horizontal component of the field B_h.

Figure 10. Fluxes of radiation, convection, and Alfven waves as functions of depth in a spot with B = 3000 gauss, and efficiency factor $\epsilon = 5$.

Figure 11. Effective temperature (solid curve, left-hand scale) and difference in temperature between solar model and sunspot model (dashed curve, right-hand scale) as functions of depth. The sunspot has B = 3000 gauss and efficiency factor $\epsilon = 5$.

Figure 12. Ratio of lateral influx of radiation from the walls of the spot at depth Z_A to the vertical flux of energy (radiative plus convective) at Z_A. Spots with small values for this ratio are expected to live longest (other things being equal). This may explain why magnetic fields in spot tend to cluster around 2000-3000 gauss. If radiative influx is responsible for setting a lower limit of 1200 gauss on spot fields, then there is also an upper limit of 5300 gauss.

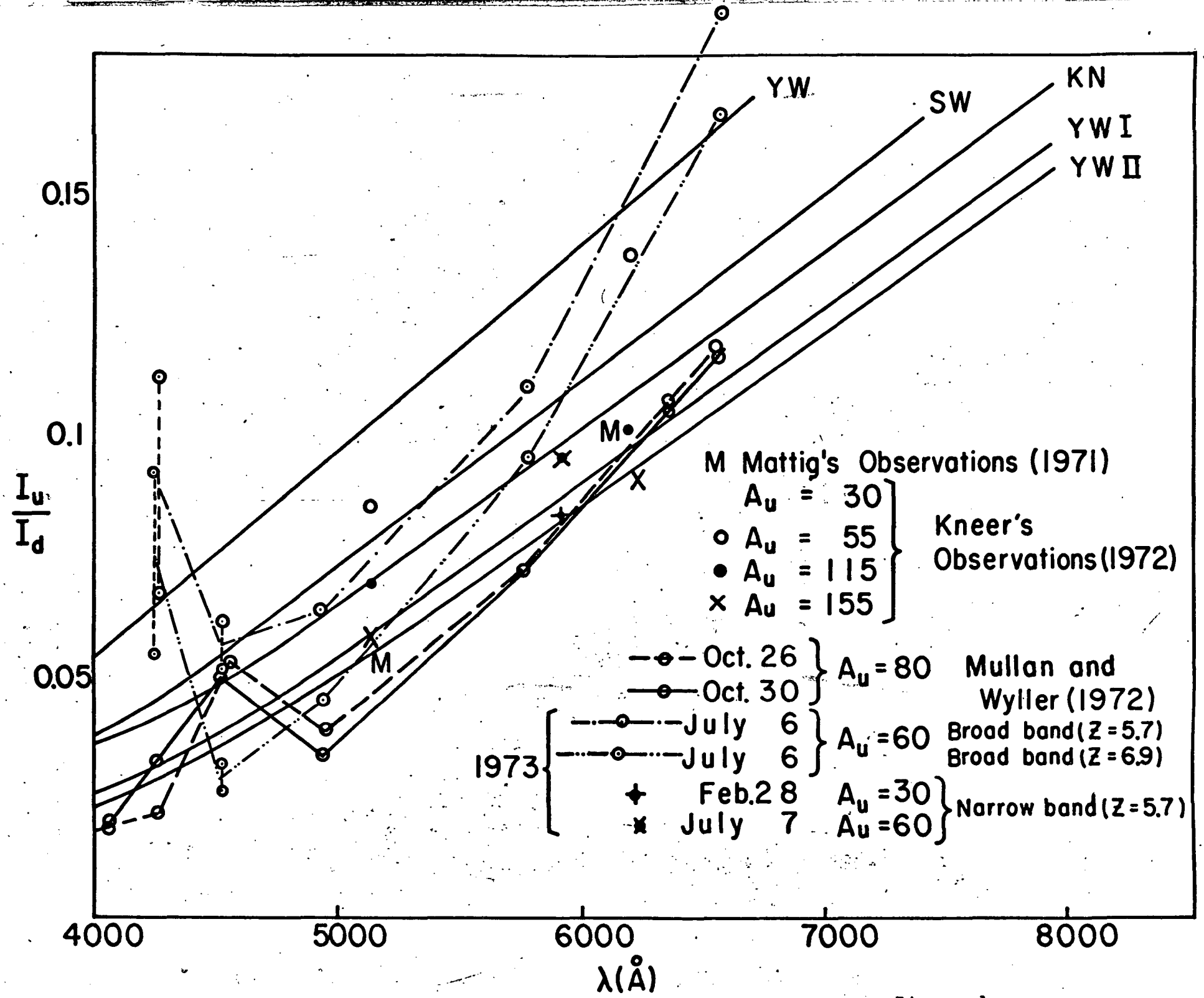
YW
SW
KN
YW I
YW II
0.15
0.1
0.05
$\frac{I_u}{I_d}$
M
M
X
M Mattig's Observations (1971)
A_u = 30
A_u = 55
A_u = 115
A_u = 155
Kneer's Observations (1972)
Oct. 26
Oct. 30
A_u = 80
Mullan and Wyller (1972)
1973
July 6
July 6
A_u = 60
Broad band (Z = 5.7)
Broad band (Z = 6.9)
Feb. 28
July 7
A_u = 30
A_u = 60
Narrow band (Z = 5.7)
4000
5000
6000
7000
8000
λ(Å)

Figure 1

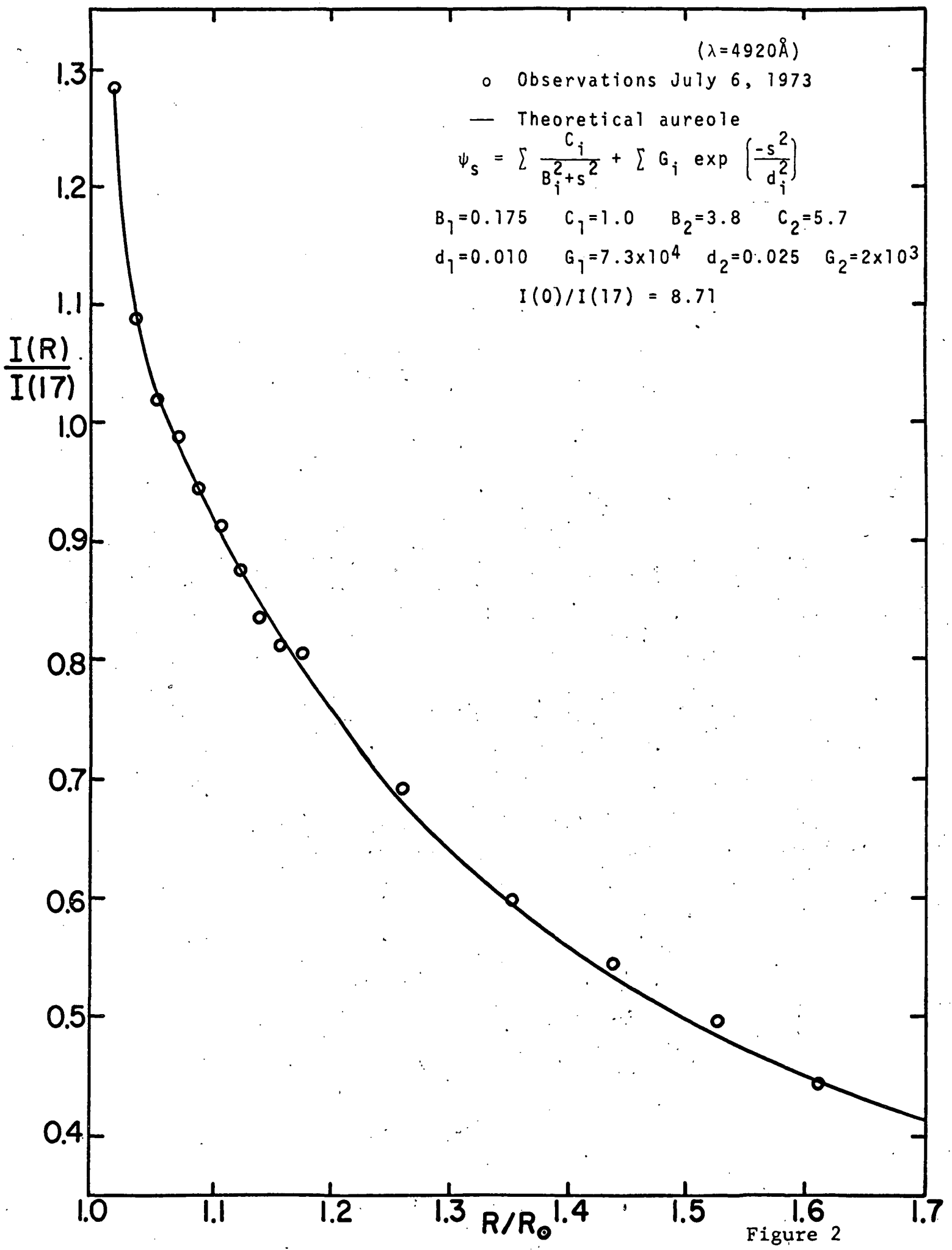
(λ=4920Å)
o Observations July 6, 1973
— Theoretical aureole
$\psi_s = \sum \frac{C_i}{B_i^2+s^2} + \sum G_i \exp\left(\frac{-s^2}{d_i^2}\right)$
$B_1=0.175$ $C_1=1.0$ $B_2=3.8$ $C_2=5.7$
$d_1=0.010$ $G_1=7.3\times10^4$ $d_2=0.025$ $G_2=2\times10^3$
I(0)/I(17) = 8.71
I(R)/I(17)
1.3
1.2
1.1
1.0
0.9
0.8
0.7
0.6
0.5
0.4
1.0
1.1
1.2
1.3
R/R⊙
1.4
1.5
1.6
1.7

Figure 2

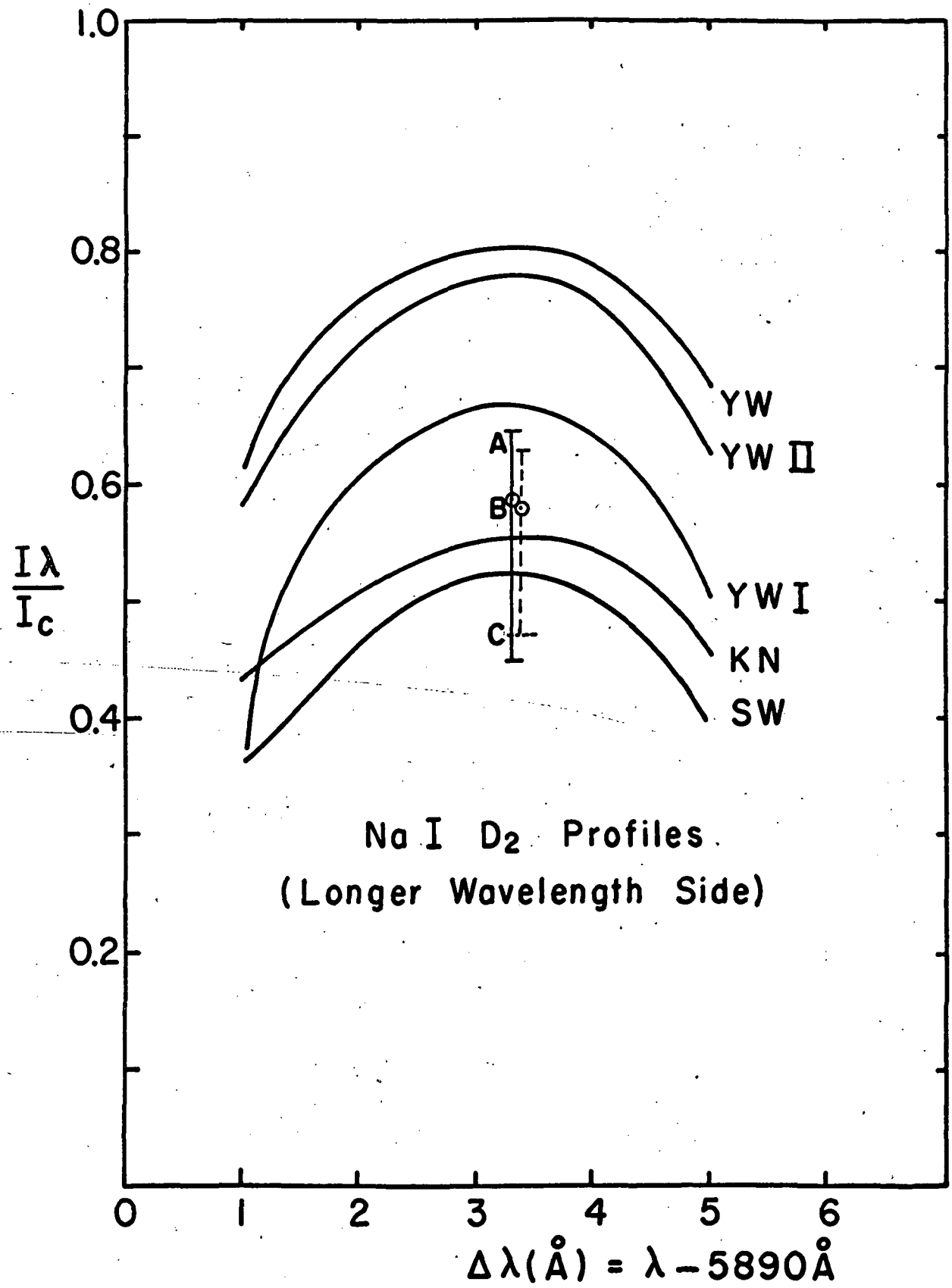
1.0
0.8
0.6
0.4
0.2
$\frac{I\lambda}{I_c}$
YW
YW II
YW I
KN
SW
A
B
C
Na I D_2 Profiles
(Longer Wavelength Side)
0
1
2
3
4
5
6
$\Delta\lambda(\text{Å}) = \lambda - 5890\text{Å}$

Figure 3

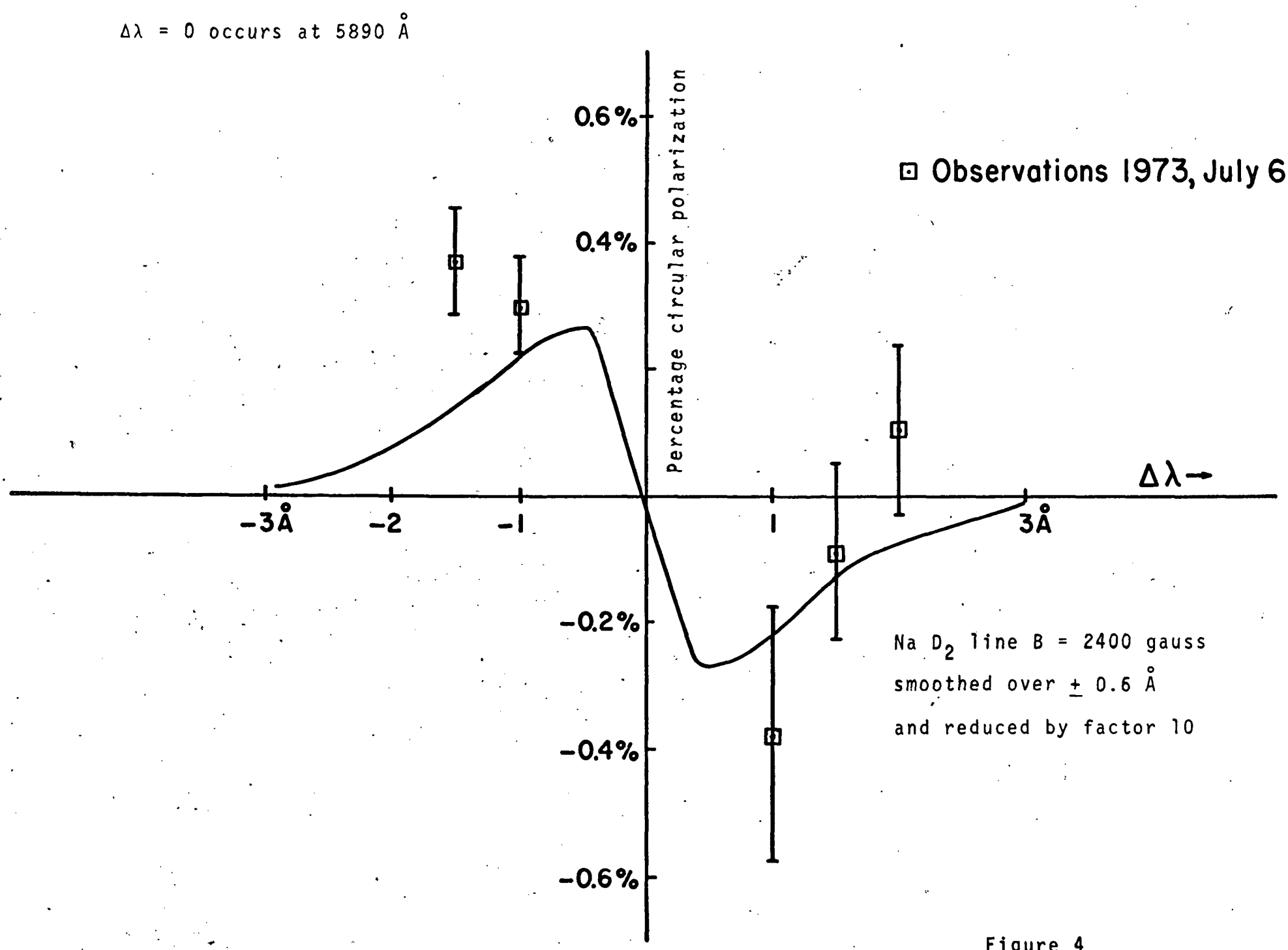
Δλ = 0 occurs at 5890 Å
Percentage circular polarization
0.6%
0.4%
-0.2%
-0.4%
-0.6%
-3Å
-2
-1
1
3Å
Δλ→
⊡ Observations 1973, July 6
Na D2 line B = 2400 gauss
smoothed over ± 0.6 Å
and reduced by factor 10

Figure 4

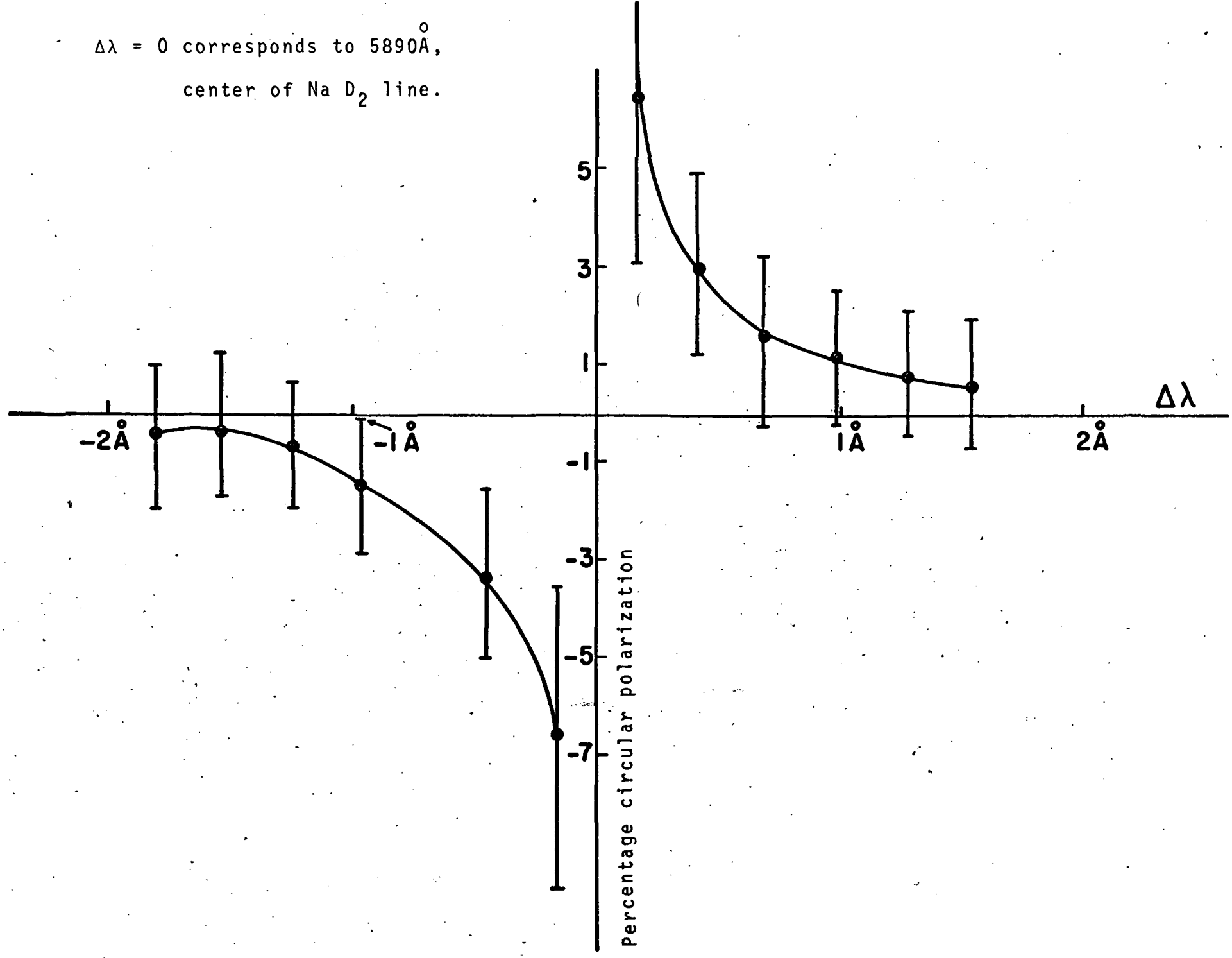
Δλ = 0 corresponds to 5890Å,
center of Na D_2 line.
5
3
1
-1
-3
-5
-7
Δλ
-2Å
-1Å
1Å
2Å
Percentage circular polarization

Figure 5

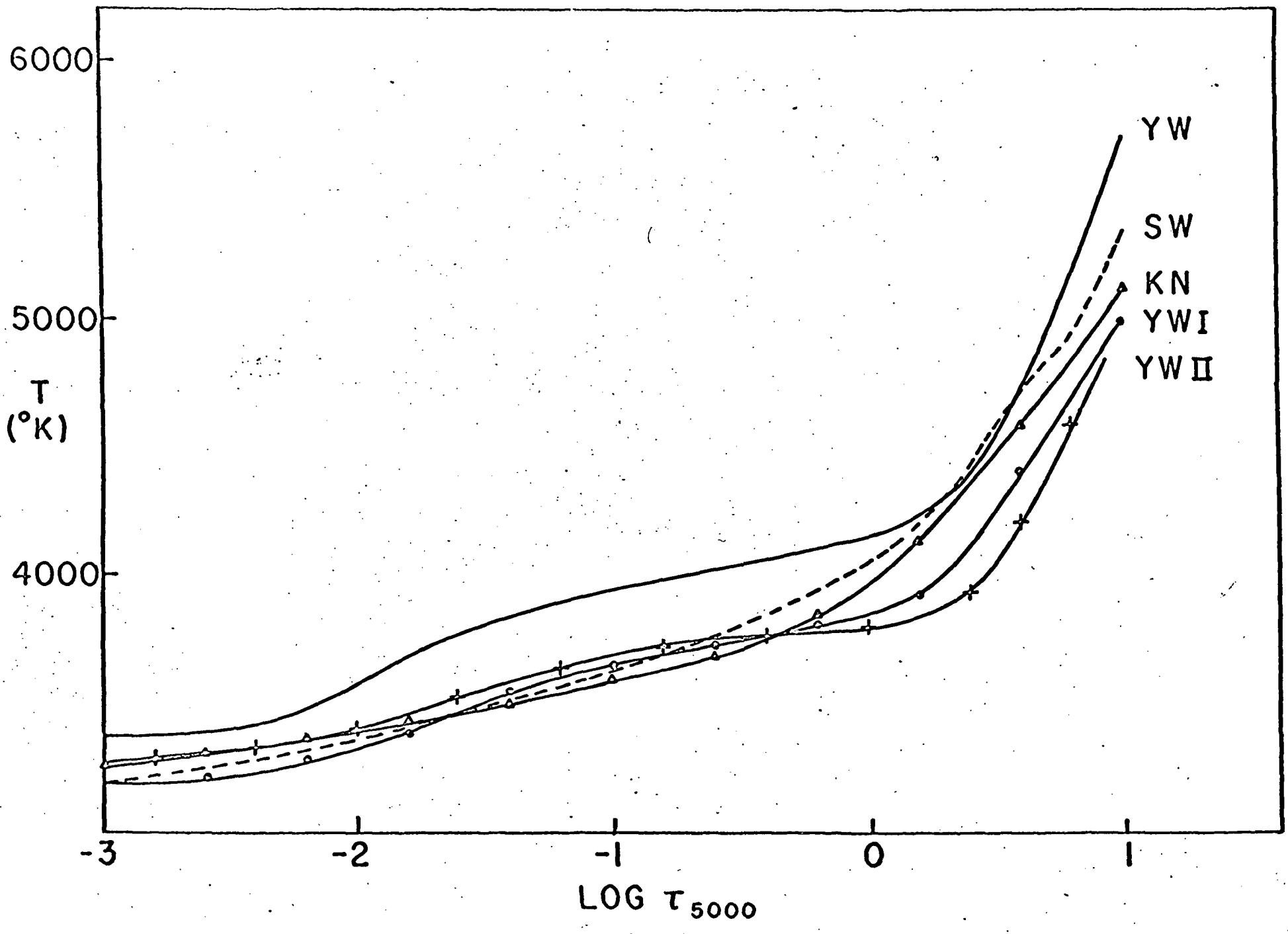

Figure 6

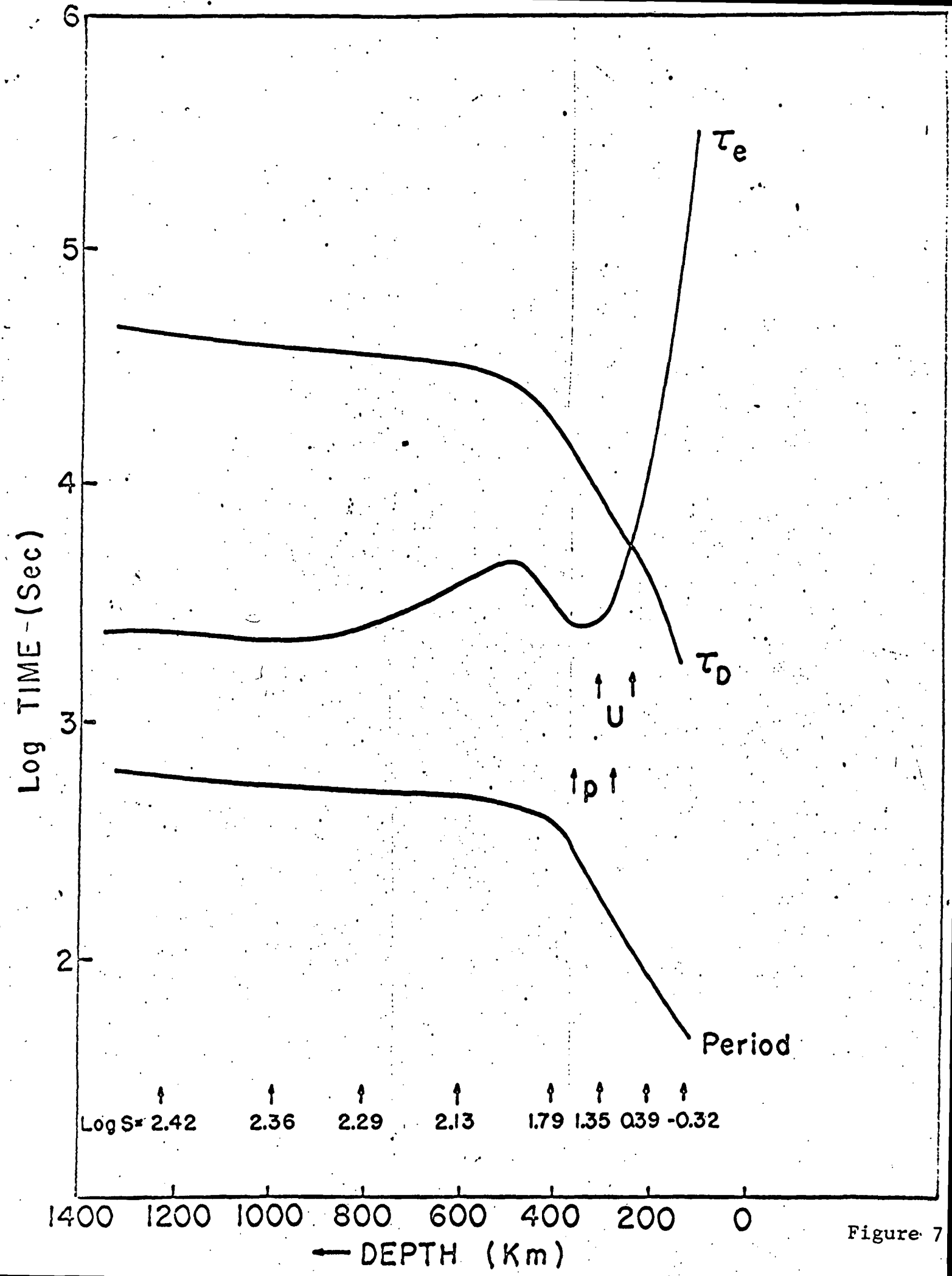
6
5
4
3
2
Log TIME-(Sec)
τ_e
τ_D
U
p
Period
Log S= 2.42
2.36
2.29
2.13
1.79
1.35
0.39
-0.32
1400
1200
1000
800
600
400
200
0
DEPTH (Km)

Figure 7

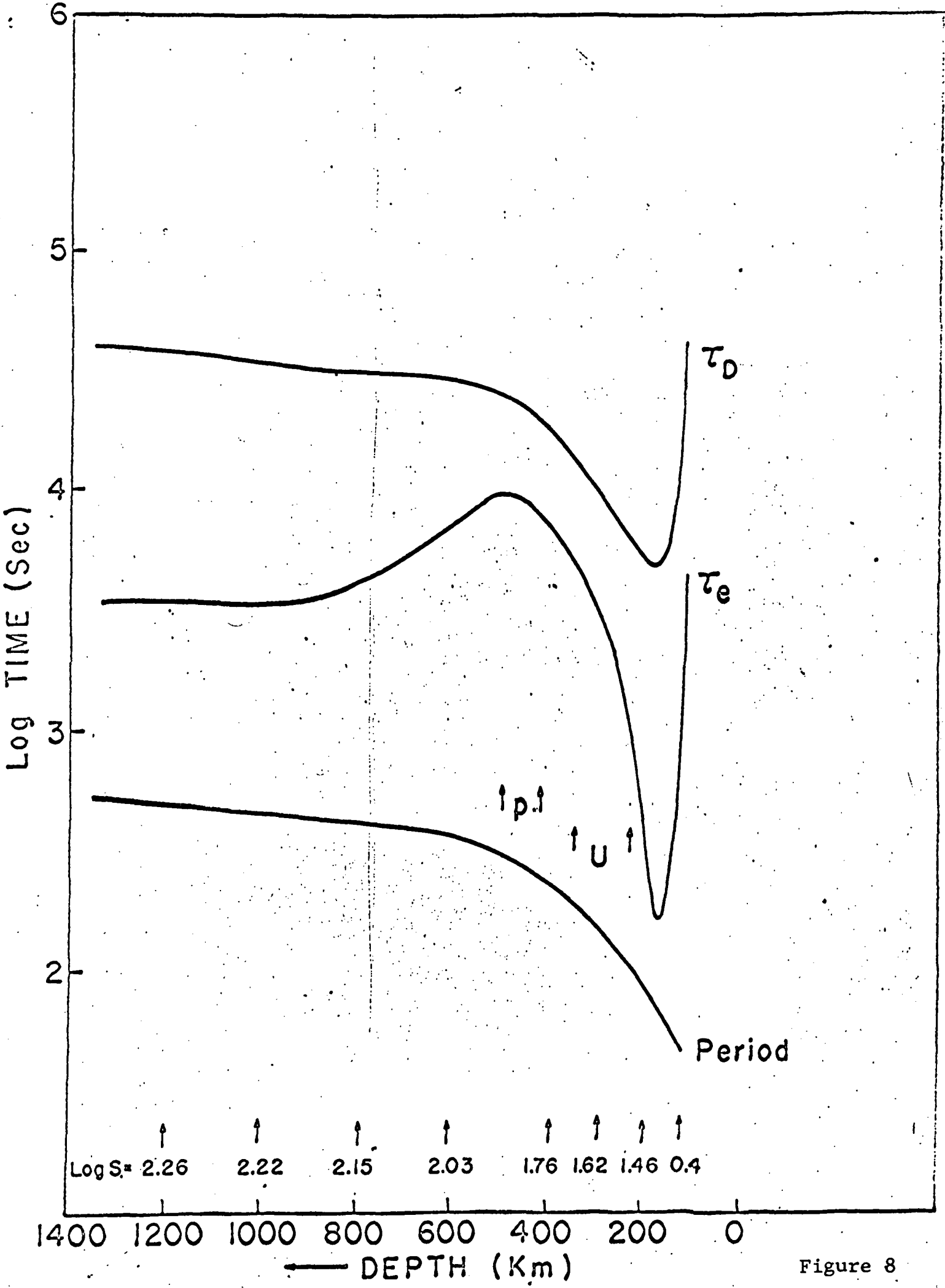
6
5
4
3
2
Log TIME (Sec)
τ_D
τ_e
p
U
Period
Log S= 2.26
2.22
2.15
2.03
1.76
1.62
1.46
0.4
1400
1200
1000
800
600
400
200
0
DEPTH (Km)

Figure 8

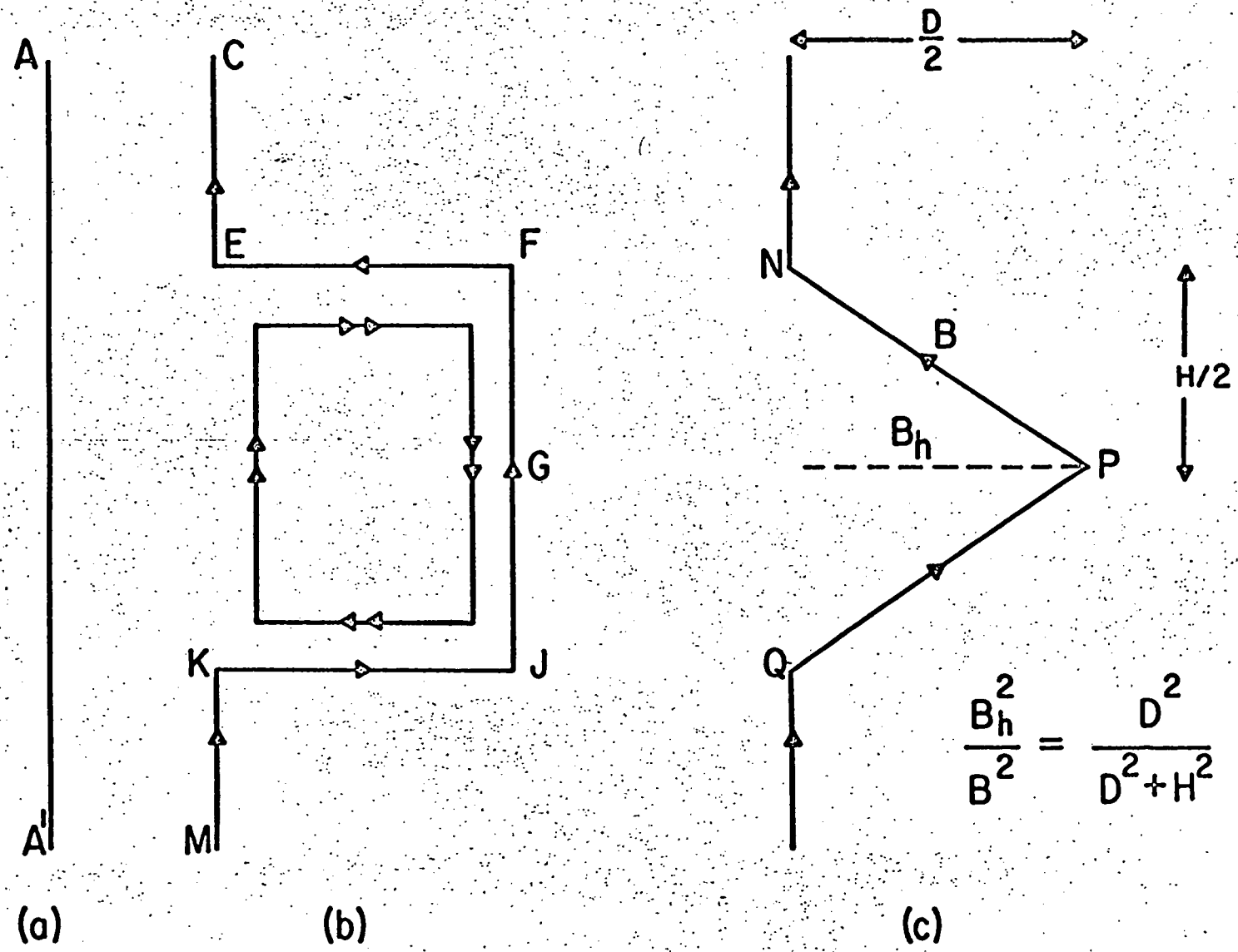

Figure 9

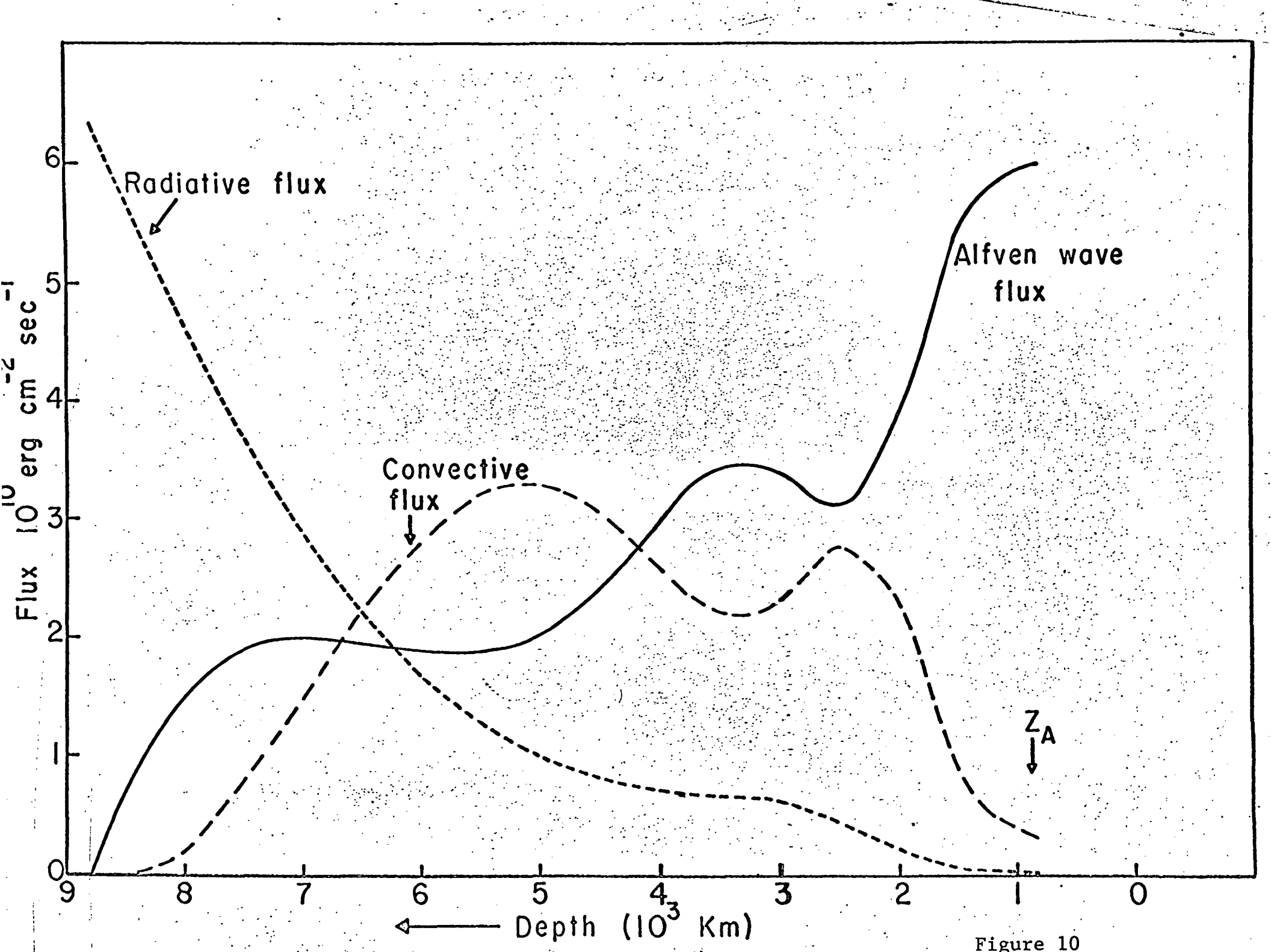
Radiative flux
Convective flux
Alfven wave flux
Z_A
Flux 10^{10} erg cm^{-2} sec^{-1}
0
1
2
3
4
5
6
9
8
7
6
5
4
3
2
1
0
Depth (10^3 Km)

Figure 10

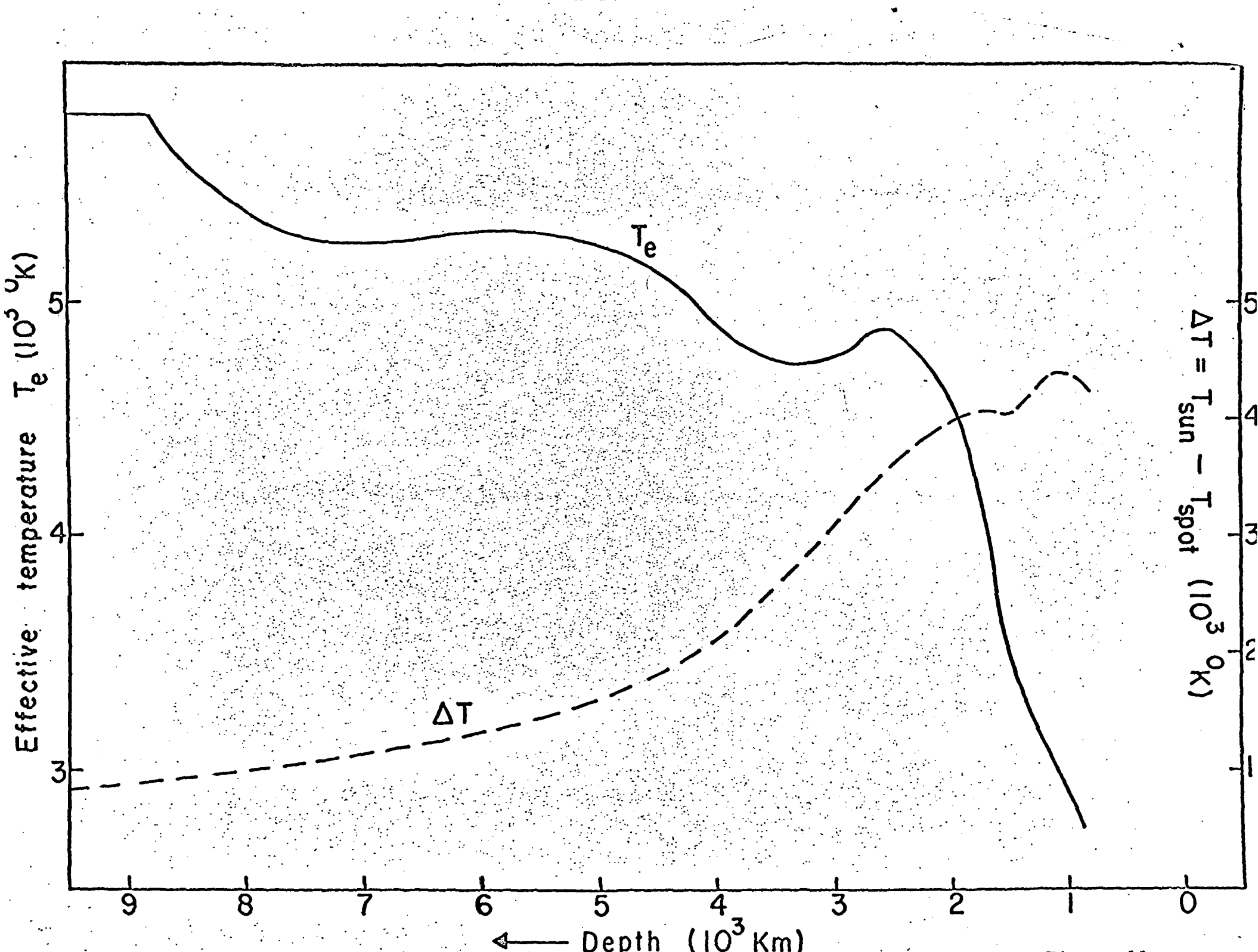
Effective temperature T_e (10^3 °K)
T_e
ΔT
$\Delta T = T_{sun} - T_{spot}$ (10^3 °K)
5
4
3
2
1
9
8
7
6
5
4
3
2
1
0
← Depth (10^3 Km)

Figure 11

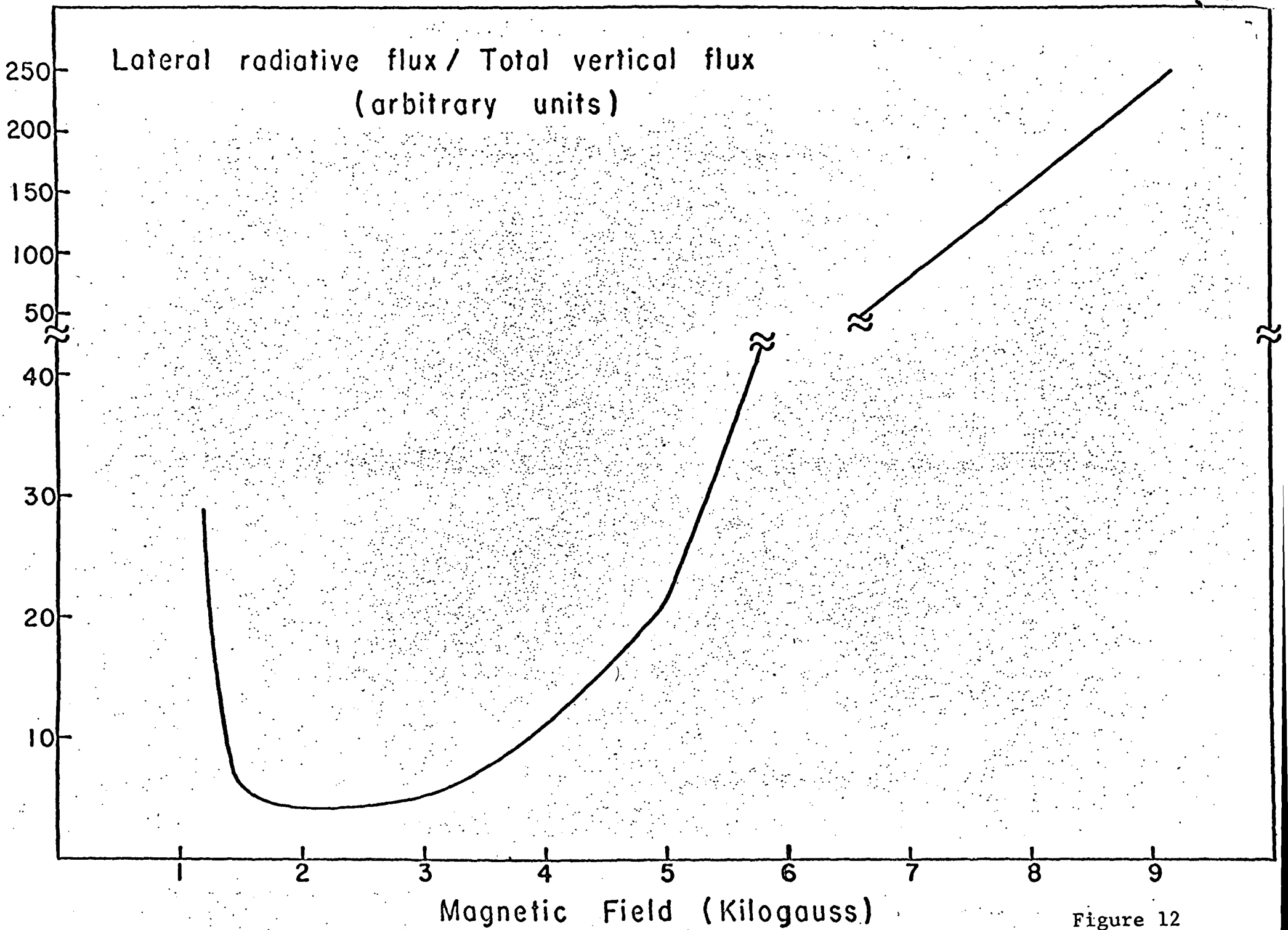
Lateral radiative flux / Total vertical flux
(arbitrary units)
250
200
150
100
50
40
30
20
10
1
2
3
4
5
6
7
8
9
Magnetic Field (Kilogauss)

Figure 12